Journal Name

ARTICLE

An investigation on the second-order nonlinear optical response of cationic bipyridine or phenanthroline iridium(III) complexes bearing cyclometallated 2-phenylpyridines with a triphenylamine substituent

Received 00th January 20xx,
Accepted 00th January 20xx

DOI: 10.1039/x0xx00000x

www.rsc.org/

Claus Hierlinger,[a,b] David B. Cordes,[b] Alexandra M. Z. Slawin,[b] Alessia Colombo,[c,d] Claudia Dragonetti*,[c,d] Stefania Righetto,[c] Dominique Roberto,[c,d] Denis Jacquemin*,[e] Eli Zysman-Colman*[b] Véronique Guerchais*[a]

The synthesis and characterisation of six new cationic iridium(III) complexes bearing either 4,4'-di*tert*-butyl-2,2'-bipyridine (d*t*Bubpy) or 5-NO_2-1,10-phenanthroline along with two cyclometallated 2-phenylpyridine derivative ligands, decorated with triphenylamine groups either *meta* or *para* to Ir-C_{C^N} bond or *para* to Ir-N_{C^N} bond, are reported. The second-order nonlinear optical (NLO) properties of all the compounds have been determined by the Electric Field Induced Second Harmonic generation technique and show that the $\mu\beta_{EFISH}$ value can be tuned by the nature of the iridium coordination sphere. The dipole moment, μ, necessary to evaluate the quadratic hyperpolarizability β_{EFISH}, was theoretically determined. The linear optical properties of the complexes are also presented and rationalised by quantum-chemical calculations. One of the prepared iridium compounds was incorporated into a polystyrene film, affording the first example of a second-order NLO active polymeric film based on a cationic organometallic complex.

Introduction

Compounds with second-order nonlinear optical (NLO) properties are useful chemical building blocks for applications in optical communications, optical data processing and storage, or optoelectronic devices.[1-2] In particular, coordination compounds are of great interest due to the presence of low-lying charge-transfer transitions between a combination of the metal and the ligands. These transitions can induce large NLO responses and can be tuned by the nature, oxidation state, and coordination sphere of the metal centre.[3-11] Such metal complexes, thanks to multiple transition with large oscillator strength, low bandgap, high dipole moment, have also been used with success in the framework of 3rd order NLO, notably in the framework of two-photon fluorescence imaging.[12-17]

Remarkably, the second-order NLO response of substituted phenylpyridines (ppy) increases significantly upon cyclometallation, an effect that has led to cyclometallated Ru(II),[18] Ir(III)[19-30] and Pt(II)[29,31-37] complexes characterised by valuable NLO properties, as measured by the Electric Field Induced Second Harmonic generation (EFISH) technique.[38-40]

More specifically, cationic cyclometallated iridium(III) complexes with π-delocalised ancillary ligands such as bipyridines[24,30] or phenanthrolines[19-23] were found to present a large second-order NLO response. For instance, [Ir(C^N)$_2$(5-R-1,10-phenanthroline)][PF_6] (C^N is a cyclometallated ligand such as phenylpyridinato (ppy) and R = H, Me, NMe_2, NO_2) show large negative second-order responses ($\mu\beta_{EFISH}$ ranging from -1270 to -2230 x 10^{-48} esu, in CH_2Cl_2).[19] The highest absolute $\mu\beta_{EFISH}$ value reported to date is that of the complex carrying a phenanthroline with the strongly electron-withdrawing NO_2 group, which confers a very strong accepting character of the π^* antibonding orbitals of the ancillary ligand. A theoretical investigation confirmed that the second-order NLO response of these Ir(III) complexes is mainly controlled by the metal-to-

[a] Univ Rennes, CNRS, ISCR (Institut des Sciences Chimiques de Rennes) – UMR 6226, F-35000 Rennes, France E-mail: veronique.guerchais@univ-rennes1.fr; Tel: + 33 (0)2 23 23 67 29.
[b] Organic Semiconductor Centre, EaStCHEM School of Chemistry, University of St Andrews, St Andrews, Fife, KY16 9ST, UK. E-mail: eli.zysman-colman@st-andrews.ac.uk; Web: http://www.zysman-colman.com; Tel: +44 (0)1334 463826.
[c] Dipartimento di Chimica dell'Università degli Studi di Milano, UdR-INSTM, via Golgi 19, I-20133, Milano, Italy. E-mail: claudia.dragonetti@unimi.it; Tel:+39 02 50314425.
[d] ISTM-CNR, CIMAINA and SmartMatLab dell'Università degli Studi di Milano, via Golgi 19, I-20133, Milano, Italy.
[e] UMR CNRS 6230, Université de Nantes, CEISAM, 2 rue de la Houssinière, 44322 Nantes Cedex 3, France. Denis.Jacquemin@univ-nantes.fr

Electronic Supplementary Information (ESI) available:

†Electronic supplementary information (ESI) available: Single-crystal X-ray analysis of **3a**, photoluminescence spectrum and photophysical data of **3a**. Additional theoretical data.

CCDC 1817920. See DOI: 10.1039/x0xx00000X

ligand/ligand-to-ligand charge transfer (MLCT/LLCT) transitions from the HOMO, located on the phenyl ring and Ir-based donor orbitals of the C^N ligands, to the LUMO localised on the π* acceptor orbitals of the phenanthroline.[19] Such an interesting effect of using the 5-NO_2-1,10-phenanthroline ligand on the NLO response was confirmed for neutral Ru(II)[40] complexes. Similarly, the use of substituted 2,2'-bipyridines instead of 1,10-phenanthrolines leads to a high NLO response as a result of the change of energy of the π* LUMO.[24,30] For instance, [Ir(C^N)$_2$(4,4'-dimethyl-2,2'-bipyridine][PF_6] is characterised by a $\mu\beta_{EFISH}$ value of -1420 x 10^{-48} esu, in CH_2Cl_2,[24] only slightly smaller than the one of the corresponding 5-Me-1,10-phenanthroline complex (-1565 x 10^{-48} esu).[19] In this kind of cationic iridium(III) complex, substitution of the ppy ligands with the more π–delocalised 2-phenylquinolinato (pq) ligands does not significantly affect the NLO properties, while a lower NLO response is observed for the related complexes with 3'-(2-pyridyl)-2,2':5',2''-terthiophene (ttpy) C^N ligands since the structure of ttpy induces a significant stabilisation of the HOMO energy, compared to the complexes bearing ppy and pq.[22] Cationic Ir(III) complexes bearing two π-delocalised cyclometallated 4-R-2-phenylpyridines (R = CH=CH-$C_6H_4NEt_2$) and a 4,4'-R',R'-2,2'-bipyridine (R' = H, Me) ancillary ligand are characterised by a $\mu\beta_{EFISH}$ value (-960 x 10^{-48} esu),[30] almost twice that reported[26] for the related cyclometallated complex with acetylacetonate as the ancillary ligand, suggesting that substitution of acetylacetonate with a 2,2'-bipyridine is a valuable strategy to increase the second-order NLO properties of the Ir(III) complexes.[30]

These results prompted us to investigate the second-order NLO properties of a family of cationic Ir(III) complexes with cyclometallated 2-phenylpyridines bearing a triphenylamino (TPA) substituent, where π-delocalisation could enhance the NLO response, partnered with 4,4'-di*tert*butyl-2,2'-bipyridine (d*t*Bubpy) and 5-NO_2-1,10-phenanthroline (NO_2-phen) as the ancillary ligands. The NLO responses of the prepared and characterised complexes **1**-**3** (**a** = d*t*Bubpy, **b** = NO_2-phen) (Chart 1) were determined by the EFISH technique,[38-39] working in $CHCl_3$ with a non-resonant incident wavelength of 1907 nm, whose second harmonic (953 nm) is in a transparent region of the absorption spectra of the compounds. The nano-organisation of this kind of complexes in a polymeric matrix was investigated as well to obtain insights regarding the solid-state response used in downstream applications.[7]

Experimental

General comments.

All reagents were purchased from Sigma-Aldrich and were used as supplied. Reactions requiring anhydrous or oxygen-free conditions were performed under nitrogen, using standard Schlenk techniques. Flash column chromatography was performed using silica gel (Silia-P from Silicycle, 60 Å, 40-63 µm). Analytical thin layer chromatography (TLC) was performed with silica plates with aluminium backings (250 µm with indicator F-254). Compounds were visualised under UV light. ^1H, ^{13}C and ^{31}P spectra solution-phase NMR spectra were recorded on a Bruker Avance spectrometer operating at 11.7 T (Larmor frequencies of 500, 126 and 162 MHz, respectively) or on a Bruker Avance-400 instrument. Chemical shifts (*δ)* are expressed in ppm relative to internal Me_4Si as standard. Signals are abbreviated as s, singlet; bs, broad singlet; d, doublet; t, triplet; q, quartet; m, multiplet. The UV-Vis spectra of the samples in dichloromethane solution were recorded using a Shimadzu UV-3150 spectrometer with 1 cm quartz cells. ESI mass spectra were measured with a LCQ fleet ion trap mass Spectrometer (ESI-MS). High-resolution mass spectra were recorded at the EPSRC UK National Mass Spectrometry Facility at Swansea University on a quadrupole time-of-flight (ESI-Q-TOF), model ABSciex 5600 Triple TOF in positive electrospray ionisation mode and spectra were recorded using sodium formate solution as the calibrant. Elemental analyses were performed by Mr. Stephen Boyer, London Metropolitan University and by Mr Mario Rosa, Università degli Studi di Milano, with a PerkinElmer CHN 2400 instrument.

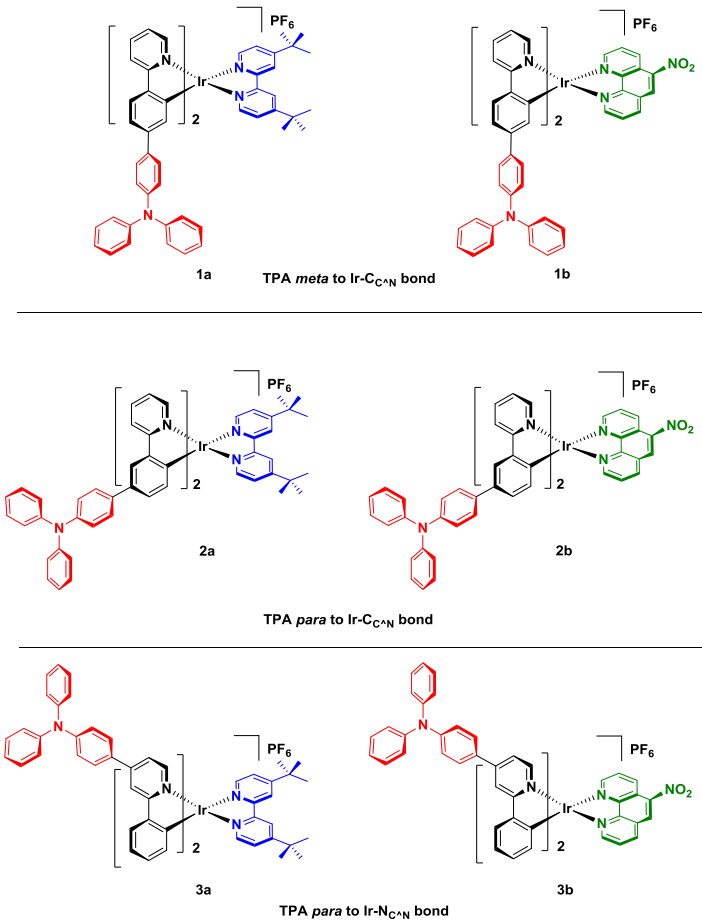

Chart 1 Complexes investigated in this study.

Synthesis of pro-ligands.

5-Nitro-1,10-phenthroline and 4,4'-di*tert*-butyl-2,2'-bipyridine are commercial. The 2-phenylpyridines substituted with a triphenylamine (TPA) **L1-L3** (Chart S1 in ESI†) were prepared through cross-coupling reactions using the appropriate bromo-substituted 2-phenylpyridines namely 2-(4-bromophenyl)pyridine,[42] 2-(3-bromophenyl)pyridine),[43] and (4-(diphenylamino)phenyl)boronic acid, which were prepared

according to the literature. Likewise, the pro-ligand **L1**[44] and the 4-bromo-2-phenylpyridine[45] precursor were synthesised according to published procedures.

General procedure for pro-ligands

A mixture of the corresponding bromo-substituted 2-phenylpyridine (1.0 equiv.), (4-(diphenylamino)phenyl)boronic acid (1.5 equiv.), 2 M aqueous K_2CO_3 (5.0 equiv.) and 1,4-dioxane (25 mL) was degassed by bubbling argon through the solution for 15 min. $Pd(PPh_3)_4$ (0.05 equiv.) was added, and the reaction mixture was heated and kept at reflux, resulting in the colour to change from yellow to brown. After 18 h the solution was allowed to cool to room temperature and the solvent was removed, leaving a brown residue, which was dissolved in EtOAc (30 mL) and washed with water. After layer separation, the combined organic layers were washed with brine (10 mL) and dried over $MgSO_4$. The solvent was evaporated leaving a brown residue, which was purified by column chromatography on silica (10 vol.% of EtOAc in petroleum ether) and the solvent was reduced to dryness leaving the desired product.

***N,N*-diphenyl-3'-(pyridin-2-yl)-[1,1'-biphenyl]-4-amine (L2):** Brown solid. Yield: 94%. R_f: 0.28 (10% of EtOAc in petroleum ether on silica). Mp.: 93-96 °C. ^{1}H NMR (400 MHz, $CDCl_3$) δ (ppm): 8.75 (dt, J = 4.8, 1.5 Hz, 1H), 8.25 (t, J = 1.9 Hz, 1H), 7.96 (dt, J = 7.7, 1.5 Hz, 1H), 7.86 – 7.74 (m, 2H), 7.69 – 7.52 (m, 4H), 7.33 – 7.26 (m, 5H), 7.19 (td, J = 6.9, 3.4 Hz, 6H), 7.11 – 7.03 (m, 2H). ^{13}C NMR (101 MHz, CDCl3) δ (ppm): 157.6, 149.8, 147.8, 147.4, 141.4, 139.9, 136.9, 135.1, 129.4, 129.3, 128.4, 127.4, 125.6, 125.5, 124.5, 124.1, 123.1, 122.3, 120.9. HR-MS (FTMS$^+$): $[M]^+$ Calculated: ($C_{29}H_{22}N_2H$): 399.1856; Found: 399.1846. CHN: Calcd. for $C_{29}H_{22}N_2x1/5CH_2Cl_2$: C, 84.41; H, 5.43; N, 6.74. Found: C, 84.28; H, 5.79; N, 6.55.

***N,N*-diphenyl-4-(2-phenylpyridin-4-yl)aniline (L3)**

Brown oil. Yield: 95%. R_f: 0.63 (20% of EtOAc in petroleum ether on silica). ^{1}H NMR (400 MHz, CDCl3) δ (ppm): 8.70 (d, J = 5.2 Hz, 1H), 8.07 – 8.00 (m, 2H), 7.90 (d, J = 1.6 Hz, 1H), 7.61 – 7.55 (m, 2H), 7.53 – 7.46 (m, 2H), 7.46 – 7.38 (m, 2H), 7.35 – 7.27 (m, 5H), 7.21 – 7.11 (m, 6H), 7.12 – 7.03 (m, 2H). ^{13}C NMR (126 MHz, CDCl3) δ (ppm): 158.0, 150.0, 148.9, 148.7, 147.3, 139.6, 131.4, 129.4, 129.0, 128.8, 127.8, 127.0, 125.0, 123.6, 123.0, 119.6, 118.1. HR-MS (FTMS$^+$): $[M]^+$ Calculated: ($C_{29}H_{22}N_2H$): 399.1856; Found: 399.1844.

Synthesis of complexes 1-3

The cationic cyclometallated Ir(III) complexes **(1-3)** were prepared in two steps: (i) synthesis of the chloro-bridge dimer $[Ir(C\hat{}N)_2Cl]_2$ with the appropriate C^N ligand; (ii) bridge splitting reaction with 4,4'-di*tert*-butyl-2,2'-bipyridine (General procedure A) or with 5-nitro-1,10-phenthroline (General procedure B).

Synthesis of $[Ir(C\hat{}N)_2Cl]_2$

The $IrCl_3.6H_2O$ (2.0 equiv.) and the corresponding C^N ligand (5.0 equiv.) were suspended in a mixture of 2-ethoxyethanol/water (75/25). The mixture was heated and kept at 125 °C under stirring. After 24 h, it was allowed to cool to r.t. and distilled water (5 mL) was added. A precipitate was observed. It was washed with Et_2O, H_2O and then dried under vacuum to give the intermediate $[Ir(C\hat{}N)_2Cl]_2$ dimer complex.

General procedure A: for the synthesis of complexes 1a, 2a and 3a

A suspension of $[Ir(C\hat{}N)_2Cl]_2$ (1.0 equiv.) and 4,4'-di*tert*-butyl-2,2'-bipyridine (2.2 equiv.) in CH_2Cl_2/MeOH (1/1 v/v; 250 mL for each mmol of dimer) was kept at reflux for 18 h under stirring. The solvent was then evaporated, leaving a brown yellow residue that was purified over silica with dichloromethane and increasing percentage of methanol (0% - 8%). The desired fractions were collected and reduced to dryness giving a yellow solid, which was dissolved in methanol. An aqueous solution of NH_4PF_6 (1.00 g in 10 mL of H_2O) was slowly added. A yellow precipitate was observed. The suspension was stirred vigorously for 2 h. The precipitate was filtered off, washed with water and Et_2O, and recrystallised in a CH_2Cl_2/hexane mixture at -20 °C. After filtration, the desired compound was obtained as a yellow-brown solid.

Complex 1a: Yellow-brown solid. Yield: 92%. ^{1}H NMR (400 MHz, $CDCl_3$) δ (ppm): 8.43 – 8.38 (m, 2H), 7.89 (t, J = 7.4 Hz, 4H), 7.77 – 7.67 (m, 4H), 7.63 (d, J = 5.9 Hz, 2H), 7.37 (dd, J = 5.9, 1.8 Hz, 2H), 7.26 – 7.21 (m, 14H), 7.11 – 7.05 (m, 10H), 7.04 – 6.98 (m, 8H), 6.55 (d, J = 1.6 Hz, 2H), 1.43 (s, 18H). ^{13}C NMR (126 MHz, $CDCl_3$) δ (ppm): 167.5, 164.0, 155.9, 151.3, 149.9, 149.2, 147.7, 147.5, 142.6, 142.1, 138.1, 134.5, 129.4, 129.2, 127.6, 125.5, 125.1, 124.7, 123.6, 123.4, 123.2, 121.8, 121.1, 119.5, 35.8, 30.4. ^{31}P NMR (162 MHz, $CDCl_3$) δ (ppm): -144.6. HR-MS (FTMS$^+$): $[M]^+$ Calculated: ($C_{76}H_{66}IrN_6$): 1255.4980; Found: 1255.4974. CHN: Calcd. for $C_{76}H_{66}F_6IrN_6PxCH_2Cl_2$: C, 62.26; H, 4.61; N, 5.66. Found: C, 61.88; H, 4.35; N, 5.89.

Complex 2a: Yellow-brown solid. Yield: 86%. ^{1}H NMR (400 MHz, $CDCl_3$) δ (ppm): 8.40 (d, J = 2.0 Hz, 2H), 7.99 (d, J = 8.1 Hz, 2H), 7.92 – 7.82 (m, 4H), 7.78 (td, J = 7.8, 1.5 Hz, 2H), 7.66 (dd, J = 5.7, 1.4 Hz, 2H), 7.49 – 7.42 (m, 4H), 7.39 (dd, J = 5.9, 1.9 Hz, 2H), 7.25 (d, J = 8.4 Hz, 10H), 7.17 – 7.08 (m, 14H), 7.01 (d, J = 8.9 Hz, 4H), 6.39 (d, J = 7.9 Hz, 2H), 1.43 (s, 18H). ^{13}C NMR (126 MHz), $CDCl_3$) δ (ppm): 167.6, 164.1, 155.9, 149.8, 149.7, 149.5, 147.8, 146.9, 144.4, 138.1, 135.5, 135.1, 132.3, 129.4, 129.3, 127.3, 125.5, 124.4, 124.3, 123.9, 123.0, 122.9, 122.0, 119.6, 35.9, 30.4. ^{31}P NMR (162 MHz, $CDCl_3$) δ (ppm): -144.56. HR-MS (FTMS$^+$): $[M]^+$ Calculated: ($C_{76}H_{66}IrN_6$): 1255.4980; Found: 1255.4969. CHN: Calcd. for $C_{76}H_{66}F_6IrN_6P$: C, 65.18; H, 4.75; N, 6.00. Found: C, 64.97; H, 4.59; N, 6.17.

Complex 3a: The residue after the ion exchange required six recrystallisations.

Yellow-brown solid. Yield: 82%. ^{1}H NMR (400 MHz, $CDCl_3$) δ (ppm): 8.45 – 8.42 (m, 2H), 8.07 – 8.04 (m, 2H), 7.89 (d, J = 5.9 Hz, 2H), 7.79 – 7.74 (m, 2H), 7.60 (t, J = 7.7 Hz, 6H), 7.42 – 7.39 (m, 2H), 7.35 – 7.32 (m, 6H), 7.18 – 7.10 (m, 20H), 7.06 – 7.02 (m, 2H), 6.96 – 6.90 (m, 2H), 6.44 (d, J = 7.4 Hz, 2H), 1.46 (s, 18H). ^{13}C NMR (126 MHz, $CDCl_3$) δ (ppm): 167.61, 164.14, 155.96, 151.30, 149.97, 149.92, 149.29, 149.08, 147.03, 143.97, 132.06, 130.63, 129.67, 128.95, 128.02, 125.44, 125.34, 124.51, 124.16, 122.41, 122.37, 122.16, 120.55, 115.93, 35.90, 30.47. ^{31}P NMR (162 MHz, $CDCl_3$) δ (ppm): -144.55. HR-MS (FTMS$^+$): $[M]^+$ Calculated: ($C_{76}H_{66}IrN_6$): 1255.4980; Found: 1255.4976. CHN: Calcd. for $C_{76}H_{66}F_6IrN_6P$: C, 65.18; H, 4.75; N, 6.00 Found: C, 64.90; H, 4.68; N, 5.91.

General procedure B: for the synthesis of complexes 1b, 2b and 3b

A solution of $[Ir(C\hat{}N)_2Cl]_2$ (1.0 equiv.) and 5-NO_2-1,10-phenanthroline (2.0 equiv.) in CH_2Cl_2/MeOH (2/1 v/v; 220 mL for each mmol of iridium dimer) was heated under reflux. After 5-6 h, the orange solution was cooled to room temperature, and then a 10-fold excess of NH_4PF_6 was added. The suspension was stirred for 15 min and then filtered to remove the insoluble inorganic salts. The solvent was evaporated under reduced pressure to obtain a crude orange solid that was dissolved in CH_2Cl_2 and filtered to remove

residual traces of salts. Diethyl ether was layered onto the orange filtrate and the mixture was cooled to 0 °C for 18 h in order to allow precipitation of the desired product. After filtration, the complex was obtained pure as orange or dark yellow solid.

Complex 1b: Orange solid. Yield: 90%. ^{1}H NMR (400 MHz, CD_2Cl_2) δ (ppm): 9.33 (dd, J = 8.0 Hz, J = 4.0 Hz, 1H), 9.15 (s, 1H), 8.87 (dd, J = 8.0 Hz, J = 4.0 Hz, 1H), 8.65-8.60 (m, 2H), 8.02-8.00 (m, 4H), 7.86 (d, J= 8.0 Hz, 2H), 7.79 (t, J= 8Hz, 2H), 7.42 (d, J=8Hz, 4H), 7.33-7.28 (m, 12H), 7.12-7.02 (m, 16H), 6.93-6.91(m, 2H), 6.69 (s, 2H). ^{13}C NMR (100 MHz, CD_2Cl_2) δ(ppm): 167.4, 154.2, 152.5, 149.2, 148.7, 148.6, 148.3, 147.6, 147.5, 147.3, 145.2, 142.5, 142.4, 140.5, 138.5, 135.3, 133.8, 129.3, 128.9, 128.6, 128.1, 127.5, 127.4, 125.5, 124.8, 124.6, 124.4, 123.2, 123.1, 121.56, 120.0. ^{31}P NMR (162 MHz, CD_3CN) δ (ppm): -144.49. ESI-MS: $[M]^+$ Calculated: ($C_{70}H_{49}IrN_7O_2$): 1212.35; Found: 1212.40. CHN: Calcd. for $C_{70}H_{49}F_6IrN_7O_2P$: C, 61.94; H, 3.64; N, 7.22. Found: C, 61.98; H, 3.65; N, 7.25.

Complex 2b: Dark yellow solid. Yield: 95%. ^{1}H NMR (400 MHz, CD_2Cl_2) δ (ppm): 9.36 (dd, J = 8.1 Hz, J = 4.0 Hz, 1H), 9.16 (s, 1H), 8.89 (dd, J = 8.1 Hz, J = 4.0 Hz, 1H), 8.66-8.60 (m, 2H), 8.12 (d, J=8.1Hz, 2H), 8.04-8.00 (m, 4H), 7.85 (t, J= 8.0 Hz, 2H), 7.58 (d, J= 8Hz, 4H), 7.45-7.40 (m, 2H), 7.33-7.29 (m, 10H), 7.20-7.15 (m, 12H), 7.10(t, J= 8.0 Hz, 4H), 7.00-6.95 (m, 2H), 6.54 (d, 2H). ESI-MS: $[M]^+$ Calculated: ($C_{70}H_{49}IrN_7O_2$): 1212.35; Found: 1212.40. CHN: Calcd. for $C_{70}H_{49}F_6IrN_7O_2P$: C, 61.94; H, 3.64; N, 7.22. Found: C, 61.90; H, 3.66; N, 7.19.

Complex 3b: Orange solid. Yield: 89%. ^{1}H NMR (400 MHz, CD_2Cl_2) δ (ppm): 9.33 (d, J = 8.0 Hz, 1H), 9.15 (s, 1H), 8.86 (d, J = 8.0 Hz, 1H), 8.62-8.56 (m, 2H), 8.16 (s, 2H), 8.05-8.00 (m, 2H), 7.91 (d, J= 8.0 Hz, 2H), 7.58 (d, J=8Hz, 4H), 7.37-7.30 (m, 10H), 7.21-7.05 (m, 22H), 6.58(d, J=8Hz,2H). ^{13}C NMR (100 MHz, CD_2Cl_2) δ(ppm): 149.9, 148.3, 146.8, 131.9, 131.3, 130.7, 130.5, 129.5, 128.3, 127.8, 127.0, 125.5, 125.2, 124.8, 124.2, 123.5, 123.1,121.9, 121.7, 120.7, 120.3, 119.6, 116.4, 114.0, 131.9, 131.3, 129.5, 127.8, 125.5, 125.2, 124.2, 123.1, 121.7, 120.3, 116.4. ^{31}P NMR (162 MHz, CD_3CN) δ (ppm): -144.50. ESI-MS: $[M]^+$ Calculated: ($C_{70}H_{49}IrN_7O_2$): 1212.35; Found: 1212.49. CHN: Calcd. for $C_{70}H_{49}F_6IrN_7O_2P$: C, 61.94; H, 3.64; N, 7.22. Found: C, 61.96; H, 3.64; N, 7.26.

EFISH measurements

EFISH measurements were carried out in $CHCl_3$ solutions at a concentration of 10^{-3} M, with a non-resonant incident wavelength of 1.907 μm, obtained by Raman-shifting the fundamental 1.064 μm wavelength produced by a Q-switched, mode-locked Nd^{3+}:YAG laser manufactured by Atalaser. The $\mu\beta_{EFISH}$ values reported are the mean values of 16 measurements performed on the same sample.

Preparation of composite films.

Thin films of complex **2b** (5% w/w relative to the polymer) dispersed in poly(methyl methacrylate) (PMMA) or polystyrene (PS) were prepared by spin-coating a few drops of a dichloromethane solution on ordinary non-pre-treated glass substrates (thickness 1 mm), previously cleaned with water/acetone. The spinning parameters were set at the following values: RPM 1 = 800; ramp 1 = 1 s, time 1 = 5 s; RPM 2 = 2000; ramp 2 = 4 s, time 2 = 83 s.

Corona Poling Setup and SHG measurements.

The fundamental incident light was generated by a 1064 nm Q-switched Nd:YAG laser. The output pulse was attenuated to 0.5 mJ and was focused on the sample, placed over the hot stage. The fundamental beam was polarised in the incidence plane (p-polarised) with an incidence angle of 55° respect to the sample. A corona-wire voltage (up to 10 kV across a 10 mm gap) was applied. After rejection of the fundamental beam by an interference filter and a glass cutoff filter, the p-polarised SHG signal at 532 nm was detected with a UV-vis photomultiplier (PT). The output signal from the PT was set to a digital store oscilloscope and then processed by a computer. Then, in the Maker fringe experiment, the second harmonic (SH) intensity was detected as a function of the incidence angle of the fundamental beam and normalised with respect to that of a calibrated quartz crystal wafer (X-cut) 1 mm thick whose d_{11} is 0.46 pm/V. The incidence angle was changed by rotating the poled film while the polarisation of the fundamental and SH beam could be changed by a half-wave plate and a cube beam splitter, respectively. In order to determine the nonzero independent components of the susceptibility tensor for poled films Maker fringe measurements were conducted with polarisations p → p, s → p, and 45 → s (where p and s indicate the polarisation of the beam in the plane parallel and orthogonal to the incident one, respectively).[46,47]

Computational details.

To perform our simulations, we have selected the Gaussian16 program.[48] The *ab initio* simulations consisted in DFT geometry optimisation, subsequent TD-DFT calculations of the different structures and determination of the dipole moments. We have applied default procedures, integration grids, algorithms and parameters, except for tighten energy (typically 10^{-8} *a.u.*) and mean internal force (10^{-5} *a.u.*) convergence thresholds and the use of the *ultrafine* integration DFT grid. The ground-state geometrical parameters have been determined with the M06 exchange-correlation functional.[49] The vibrational spectrum has been subsequently determined analytically at the same level of theory and it has been checked that all structures correspond to true minima of the potential energy surface. At least, the first forty low-lying excited-states have been determined within the vertical TD-DFT approximation using the same functional, that is also suited for absorption spectra.[50] Finally, the dipole moments have been computed using a range-separated hybrid with a correct asymptotic behaviour for electron-electron interactions, namely ωB97X-D.[51] For all nuclei, we have used the LanL2DZ(5*d*,7*f*) basis set and pseudopotential augmented by additional *d* (C, N) and *f* (Ir) functions of contraction length one (α=0.938, 0.587, 0.961 and 0.648 for C, N, O, and Ir, respectively). During all steps, a modelling of bulk solvent effects ($CHCl_3$) through the Polarizable Continuum Model (PCM),[52] using the linear-response non-equilibrium approach for the TD-DFT part of the calculation. As a final note, the counterions have not be accounted for in our calculations, so that the dipole moment reported below are taken at the centre of mass for all compounds.

Results and discussion

The cationic cyclometallated Ir(III) complexes (**1-3**) were prepared in two steps: (i) synthesis of the chloro-bridge dimer, $[Ir(C^N)_2Cl]_2$; (ii) bridge splitting reaction with 4,4'-di*tert*butyl-2,2'-bipyridine or with

5-nitro-phenthroline (see Experimental). All complexes were characterised by NMR spectroscopy, ESI-HR mass spectra, and elemental analysis.

Crystal structure of 3a

Single crystals of complex **3a** were grown by the slow vapour diffusion of hexane into a CH_2Cl_2 solution of the complex. The structure of **3a** was determined by single-crystal X-ray diffraction (Fig. 1, Tables S1 and S2 in ESI†).

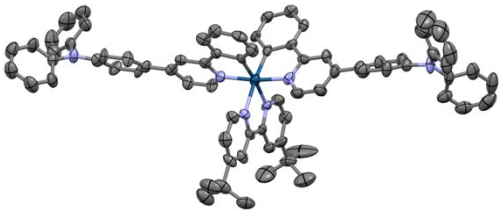

Fig. 1. Solid-state structure of complex **3a**. Thermal ellipsoids are drawn at the 50 % probability level. Hydrogen atoms, PF_6^- counterion and solvent molecules are omitted for clarity.

Complex **3a** displays a pseudo-octahedral geometry around the Ir, with the nitrogen atoms of the C^N ligands oriented in a *trans* disposition, the usual configuration in cationic Ir(III) complexes.[20,53-56] Bond lengths and bond angles are as expected for this class of iridium complex. The angles between the planes of the pyridine of the C^N ligand and the non-coordinating phenyl ring bound to it are on average 29° [16.5(6)° and 41.4(7)°], similar to the equivalent angles seen in $[Ir(DiPhPy)_2(bpy)]PF_6$[56] (where DiPhPy is 2,4-diphenylpyridinato; bearing a phenyl group *para* to Ir-N_{C^N} bond); with an average angle of 26.0° between the planes of the phenyl and the pyridine of the C^N ligands.

UV-vis Absorption

The UV-Vis absorption spectra of complexes **1-3** were recorded in $CHCl_3$ at 298 K and the data are summarised in Table 1. The absorption spectra of the six complexes are shown in Figure 2. All complexes show intense high-energy (ε on the order of 5.0 – 5.9 × 10^4 M^{-1} cm^{-1}) absorption bands below 300 nm, which are attributed to π–π* ligand-centred (^{1}LC) transitions localised on the N^N and C^N ligands. A distinguishing feature of each complex is the presence of a band at low energy, which is attributed, thanks to calculations, to an intraligand charge transfer (ILCT) from the TPA moiety to the phenyl and pyridyl rings of the C^N ligands bonded to the metal. For complexes **2a** and **2b**, this band, that appears at 435 nm, is much less intense (intensities of ε = 3.2 and 5.13 × 10^3 M^{-1} cm^{-1}, respectively) compared to the other complexes in this study. The intense absorption peaking at λ_{abs} of 333 and 327 nm (ε ~ 5.2 × 10^4 M^{-1} cm^{-1}), for **2a** and **2b**, respectively present a strongly mixed character (ILCT/ML'CT/LL'CT), L and L' being the C^N and L' N^N ligand(s), respectively, according to calculations. Complexes **1a** and **1b** show similar profiles, with a broad and intense band presenting a λ_{abs} at 384 and 381 nm (ε ~ 4.0 × 10^4 M^{-1} cm^{-1}), respectively. The maxima of the band are even further bathochromically shifted for complexes **3a** (λ_{abs} = 403 nm) and **3b** (λ_{abs} = 413 nm) and the intensity of the band is enhanced as well with ε ~ 5.4 × 10^4 M^{-1} cm^{-1}. For all complexes, weak absorption bands are observed beyond 450 nm, tailing to 590 nm. These bands are assigned to spin-forbidden transition to the triplet excited states (^{3}M'L'CT/^{3}LL'CT).

Table 1 Main absorption bands in the UV-visible spectra, dipole moments and second-order NLO response.

	Absorption[a] λ_{max} / nm (ε / M^{-1} cm^{-1})	**μβ$_{EFISH}$**[a,b] / × 10^{-48} esu	**μ**[c] / D	**β$_{EFISH}$**[d] / × 10^{-30} esu
1a	280 (55 393), 294 (55 813), 384 (43 488), 426 (19 538)	-1260	19.8	-64
1b	270 (56 011), 293 (50 418), 381 (38 389), 426 (20 927)	-1370	14.2	-96
2a	279 (50 209), 333 (52 526), 435 (3 200)	-1560	23.6	-66
2b	271 (59 488), 327 (53 387), 435 (5 133)	-1730	19.6	-88
3a	295 (53 726), 403 (54 042)	-1880	12.0	-157
3b	273 (59 105), 413 (54 816)	-1890	6.4	-295

(a) In $CHCl_3$. (b) at 1.907 μm; estimated uncertainty in EFISH measurements is ±10%. (c) computed dipole moments of the cationic iridium complex using PCM-DFT (see Experimental Section for details). (d) β_{EFISH} calculated using the computed μ value.

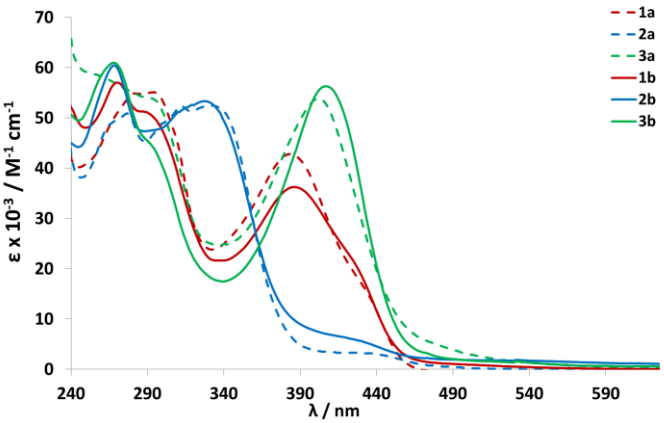

Fig. 2 UV-vis absorption spectra of **1a-3a** (in dashed lines) **1b-3b** (in solid lines) in $CHCl_3$ at 298 K

We have used TD-DFT to provide insights into the nature of the low-lying excited-states of the complexes in this study. The results are detailed in the ESI. As can be seen in Fig. S3 (ESI†), the general shape provided by theory matches the experimental spectra, with, in

particular, a much less intense long-wavelength band for **2a** than for **1a** and **3a**. For **1a**, theory returns the first three lowest significantly dipole-allowed (*f*>0.1) excited-states at 440, 433, and 411 nm. These three states correspond to the experimental broad ILCT band in the visible region. In **1b**, theory returns excited-states at 449, 445, and 440 nm, slightly red-shifted compared to **1a**, which is again consistent with experiment. In **3a** and **3b**, TD-DFT returns a strong excited-state (*f* larger than 1) at 428 nm and 430 nm, other states presenting significantly smaller oscillator strengths. This is rather consistent with the experimental spectra that show slightly less broad bands in **3** than in **1**. In **2a** and **2b,** only one significantly dipole-allowed state appears above 400 nm, but the oscillator strength is much smaller than in the other complexes. The interested reader will find more information in Table S4 in the ESI†, with descriptions of the MO compositions that are generally rather complex for all states. Nevertheless, as can be seen from Table S4, the low-lying bands in **1a**, **2a** and **3a** all correspond to HOMO to LUMO+1 transitions, both orbitals being localised on the C^N ligand and displaying a very significant CT character. The LUMO, localised on the ancillary ligand is not involved in these (allowed) transitions, as HOMO to LUMO transitions present a vanishing oscillator strength due to the non-overlapping densities (Fig. S4, ESI†).

The HOMO of **3a** has a different topology and is more stabilized (-5.80 eV), compared to the HOMO of **1a** (-5.60 eV) and **2a** (-5.50 eV), consistent, with the blueshifted λ_{max} of **3a**.

In solution ($CHCl_3$ and MeCN) the complexes show very weak emission, except for complex **3a**. For this reason, only the emission properties of **3a** are discussed here. Fig. S1 (ESI†) shows the normalised photoluminescence (PL) spectrum of **3a** in degassed MeCN and the data are summarised in Table S3 (ESI†). Upon photoexcitation at 420 nm, complex **3a** exhibits a broad and featureless emission, indicative of an emission with mixed CT character, with a maximum at λ_{PL} = 573 nm and a photoluminescence quantum yield (Φ_{PL}) of 7%. Compared to the unsubstituted analogue $[Ir(ppy)_2(dtBubpy)]PF_6$[54] (λ_{PL} = 591 nm, Φ_{PL} = 29%) a blue-shift of 18 nm (532 cm^{-1}) and a notable lowering of the Φ_{PL} is observed.

NLO studies

We used the EFISH method in order to study the second-order NLO response in solution of the complexes. This technique[38-40] provides direct information on the intrinsic molecular NLO properties, through

$$\gamma_{EFISH} = (\mu\beta_{EFISH}/5kT) + \gamma(-2\omega; \omega, \omega, 0) \quad (1)$$

where $\mu\beta_{EFISH}/5kT$ is the dipolar orientational contribution to the molecular nonlinearity, and $\gamma(-2\omega; \omega, \omega, 0)$, the second hyperpolarizability, is a purely electronic third-order contribution to γ_{EFISH}, which can usually be neglected when studying the second-order NLO properties of dipolar molecules, dominated by the first hyperpolarizability. β_{EFISH} is the projection along the dipole moment axis of β_{vec}, the vectoral component of the tensor of the quadratic hyperpolarizability, working with an incident wavelength of a pulsed laser. To obtain the value of β_{EFISH}, it is therefore necessary to determine the ground state dipole moment μ of the molecule. To avoid overestimations of the β value due to resonance enhancements, it is also essential to choose an incident wavelength whose second harmonic is remote from any absorption of the molecule investigated. Besides, it is worth noting that the EFISH technique can be applied to the determination of the second-order NLO response of ionic species by working in a solvent of low dielectric constant like $CHCl_3$ which ensure tight ion-pairing.[57-58] In contrast, when using CH_2Cl_2 as solvent, it is necessary to choose carefully the counterion in order to have a tight ion-pair. For example, it was shown that the $\mu\beta_{EFISH}$ value of $[Ir(ppy)_2(5\text{-}NO_2\text{-}1,10\text{-phenanthroline})][PF_6]$ goes from -2230 x 10^{-48} esu to -1430 x 10^{-48} esu, in CH_2Cl_2, upon substitution of PF_6^- by $C_{12}H_{25}SO_3^-$, mainly due to strengthening of the ion-pair.[23] Therefore $CHCl_3$ was used as solvent to determine the second-order NLO properties of all complexes.

We found that all complexes are characterised by a negative $\mu\beta_{EFISH}$ (Table 1), in agreement with a negative value for $\Delta\mu_{eg}$, the difference of the excited and ground state dipole moments,[59] consistently with previous reports on cyclometallated Ir(III) complexes.[19-30]

Complex **1a**, where TPA is *meta* to the Ir-C_{C^N} bond, is characterised by a large second-order NLO response ($\mu\beta_{EFISH}$ = -1260 ×10^{-48} esu). A slightly higher absolute value of $\mu\beta_{EFISH}$ is observed for the related complex with the TPA substituent in position *para* to the Ir-C_{C^N} bond, **2a**. This enhancement is due to an increase of the dipole moment of the complex (Table 1). A much higher NLO response is reached with **3a** ($\mu\beta_{EFISH}$ = -1880 ×10^{-48} esu), where TPA is *para* to the Ir-N_{C^N} bond, due to a much higher quadratic hyperpolarizability, β_{EFISH}, which prevails over the decrease of the dipole moment. This decrease is due to the more symmetric arrangement of the donating groups around the metallic centre that leads to vector contributions to the dipoles in opposite directions, as clearly seen in Chart 1.

Complexes **1b-3b** possess a smaller dipole moment than their **1a-3a** analogues but they are characterised by a higher second-order NLO response due to an increase of the quadratic hyperpolarizability, as expected for the strong acceptor properties of 5-NO_2-1,10-phenanthroline (Table 1).

Although the NLO responses of these complexes in solution provide insights into molecular design, a further step is to obtain organised molecular materials showing a high second-order solid-state NLO response.[7] While some neutral organometallic compounds have been incorporated into polymeric films affording rather large second-harmonic generation (SHG) responses,[7,60-62] to the very best of our knowledge no NLO-active polymeric films based on ionic organometallic complexes has been reported. This observation prompted us to investigate the second-order NLO properties of **2b** incorporated in a polymeric film. This cationic complex was chosen because it is simultaneously characterised by one of the largest $\mu\beta_{EFISH}$ values in the series, and a significant dipole moment (Table 1), which should facilitate the orientation of the complex by poling.

Thus, we have prepared thin films of **2b** dispersed in a polymethylmethacrylate (PMMA) or polystyrene (PS) matrix, as reported in the experimental section. It turned out that the second-harmonic generation signal of films in PMMA rapidly

faded due to the loss of orientation of the dyes. A much better behaviour was obtained by using polystyrene as matrix (Figure **3**). The SHG was negligible before applying the corona voltage but it quickly increased after application of the electric field. When the temperature was increased up to 70-80 °C, a large increase of the SHG occurred, due to the decrease of the viscosity of the polymeric matrix which allowed an easier orientation of the NLO-active complex. When a stable SHG was reached, the sample was cooled at room temperature and the electric field switched off. By fitting the Maker fringe measurements,[47] the three nonzero coefficients of the second-order susceptibility tensor $\chi_{33}^{(2)}$, $\chi_{31}^{(2)}$ and $\chi_{15}^{(2)}$ for the poled film were found to be 1.7, 0.46 and 0.50 pm/V, respectively. Although this $\chi_{33}^{(2)}$ value is lower than that previously reached for a neutral cyclometallated Ir(III) complex (3.0 pm/V),[28] it remains an interesting result because it represents the first demonstration of SHG properties of a cationic organometallic complex embedded in a polymeric film.

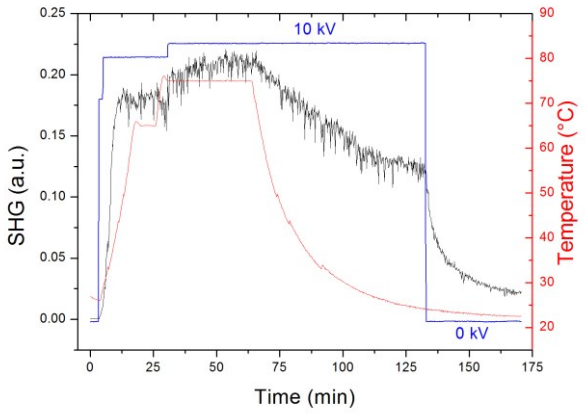

Fig. 3 Poling of the **2b**/polystyrene film. SHG (black line), temperature (red line) and electric field (blue line).

Conclusions

In summary, this work has shown the large $\mu\beta_{EFISH}$ values of six new and well characterised cationic iridium(III) complexes bearing either 4,4'-di*tert*butyl-2,2'-bipyridine or 5-NO_2-1,10-phenanthroline along with cyclometallated 2-phenylpyridines substituted with a triphenylamine in position *meta* or *para* to Ir-$C_{C\wedge N}$ bond or *para* to Ir-$N_{C\wedge N}$ bond. Remarkably, polymeric films based on this kind of cationic iridium complexes can exhibit a good second-harmonic generation response, which is particularly stable by using polystyrene as matrix. These results will stimulate further studies on polymeric films incorporating cationic complexes for NLO applications.

Acknowledgements

We deeply thank Dr Daniele Marinotto for SHG measurements and Prof. Luigi Falciola for cyclovoltammetry. This work was supported by MIUR, CNR and the National Interuniversity Consortium of Materials Science and Technology (Project INSTMMI012) in Italy. C.H. acknowledges the *Région Bretagne*, France for funding. E.Z.-C. acknowledges the University of St. Andrews and EPSRC (EP/M02105X/1) for financial support. We thank Umicore AG for the gift of materials and the EPSRC UK National Mass Spectrometry Facility at Swansea University for analytical services. This work uses computational resources of the CCIPL installed in Nantes and the GENCI consortium.

Notes and references

1 J. Zyss, *J. Molecular Nonlinear Optics: Materials, Physics and Devices*, Academic Press, Boston, 1994.
2 N. P. Prasad, and D. J. Williams, In *Introduction to Nonlinear Optical Effects in molecules and Polymers*; Wiley, 1991.
3 E. Cariati, M. Pizzotti, D. Roberto, F. Tessore, R. Ugo, *Coord. Chem. Rev.*, 2006, **250**, 1210.
4 B. J. Coe, *Acc. Chem. Res*. 2006, **39**, 383.
5 J. P. Morrall, G. T. Dalton, M. G. Humphrey, M. Samoc, *Adv. Organomet. Chem.*, 2007, **55**, 61.
6 O. Maury, H. Le Bozec, In *Molecular Materials*; Eds: D.W. Bruce, D. O'Hare, R.I. Walton, Wiley: Chichester, 2010, 1.
7 S. Di Bella, C. Dragonetti, M. Pizzotti, D. Roberto, F. Tessore, R. Ugo, In *Topics in Organometallic Chemistry 28. Molecular Organometallic Materials for Optics;* Eds: H.; Le Bozec, V., Guerchais, Springer, 2010, **28**, 1.
8 M. Pizzotti, R. Ugo, D. Roberto, S. Bruni, P. Fantucci, C. Rovizzi, *Organometallics*, 2002, **21**, 5830.
9 F. Tessore, D. Roberto, R. Ugo, P. Mussini, S. Quici, I. Ledoux-Rak, J. Zyss, *Angew. Chem. Intern. Ed.*, 2003, **42**, 456.
10 M.G. Humphrey, T. Schwich, P.J. West, M.P. Cifuentes, M. Samoc, In *Comprehensive Inorganic Chemistry II (Second Edition): From Elements to Applications*, Elsevier: Oxford, U.K. 2013; Vol 8.
11 I.P. Oliveri, S. Failla, A. Colombo, C. Dragonetti, S. Righetto, S. Di Bella, *Dalton Trans.,* 2014**, 43**, 2168.
12 A. Picot, A. D'Aleo, P.L. Baldeck, A. Grichine, A. Duperray, A. Chantal, O. Maury, *J. Am. Chem. Soc*., 2008, **130**, 1532.
13 E. Baggaley, I.V. Sazanovich, J.A.G. Williams, J.W. Haycock, S.W. Botchway, J.A. Weinstein, *RSC Advances*, 2014, **4**, 35003.
14 A. Grichine, A. Haefele, S. Pascal, A. Duperray, R. Michel, C. Andraud, O. Maury, *Chemical Science*, 2014, **5**, 3475.
15 R. Chen, J. Zhang, J. Chelora, Y. Xiong, S.V. Kershaw, K.F. Li, P.-K. Lo, K.W. Cheah, A.L. Rogach, J.A. Zapien, C.-S. Lee, *ACS Applied Materials & Interfaces*, 2017, **9**, 5699.
16 C. Jin, R. Guan, J. Wu, B. Yuan, L. Wang, J. Huang, H. Wang, L. Ji, H. Chao, *Chem. Commun*., 2017, **53**, 10374.
17 Q. Zhang, X. Lu, H. Wang, X. Tian, A. Wang, H. Zhou, J. Wu, Y. Tian, *Chem. Commun*. 2018, **54**, 3771.
18 L. Labat, J.F. Lamere, I. Sasaki, P.G. Lacroix, L. Vendier, I. Asselberghs, J. Perez-Moreno, K. Clays, *Eur. J. Inorg. Chem.,* 2006, **15**, 3105.
19 C. Dragonetti, S. Righetto, D. Roberto, R. Ugo, A. Valore, S. Fantacci, A. Sgamellotti, F. De Angelis, *Chem. Commun.*, 2007, **40**, 4116.
20 C. Dragonetti, S. Righetto, D. Roberto, R. Ugo, A. Valore, F. Demartin, F. De Angelis, A. Sgamellotti, S. Fantacci, *Inorg. Chim. Acta,* 2008*,* **361***,* 4070.
21 C. Dragonetti, S. Righetto, D. Roberto, A. Valore, *Phys. Status Solid C,* 2009, **6**, S50.

22 C. Dragonetti, S. Righetto, D. Roberto, A. Valore, T. Benincori, F. Sannicolò, F. De Angelis, S. Fantacci, *J. Mat. Sci.: Mat. Electr.*, 2009, **20**, S460.

23 A. Valore, E. Cariati, C. Dragonetti, S. Righetto, D. Roberto, R. Ugo, F. De Angelis, S. Fantacci, A. Sgamellotti, A. Macchioni, D. Zuccaccia, *Chem. Eur. J.,* 2010, **16***,* 4814.

24 V. Aubert, L. Ordronneau, M. Escadeillas, J.A.G. Williams, A. Boucekkine, E. Coulaud, C. Dragonetti, S. Righetto, D. Roberto, R. Ugo, A. Valore, A. Singh, J. Zyss, I. Ledoux-Rak, H. Le Bozec, V. Guerchais, *Inorg. Chem.,* 2011, **50***,* 5027.

25 C. Dragonetti, A. Valore, A. Colombo, S. Righetto, G. Rampinini, F. Colombo, L. Rocchigiani, A. Macchioni, *Inorg. Chim. Acta*, 2012, **382**, 72.

26 M. Zaarour, A. Singh, C. Latouche, J.A.G. Williams, I. Ledoux-Rak, J. Zyss, A. Boucekkine, H. Le Bozec, V. Guerchais, C. Dragonetti, A. Colombo, D. Roberto, A. Valore, *Inorg. Chem.,* 2013, **52**, 7987.

27 M. Zaarour, V. Guerchais, H. Le Bozec, C. Dragonetti, S. Righetto, D. Roberto, F. De Angelis, S. Fantacci, M.G. Lobello, Dalton *Trans.,* 2013, **42**, 155.

28 C. Dragonetti, A. Colombo, D. Marinotto, S. Righetto, D. Roberto, A. Valore, M. Escadeillas, V. Guerchais, H. Le Bozec, A. Boucekkine, C. Latouche, *J. Organomet. Chem.,* 2014, **751**, 568.

29 A. Valore, A. Colombo, C. Dragonetti, S. Righetto, D. Roberto, R. Ugo, F. De Angelis, S. Fantacci, *Chem. Commun.,* 2010, **46***,* 2414.

30 A. Colombo, E. Garoni, C. Dragonetti, S. Righetto, D. Roberto, N. Baggi, M. Escadeillas, V. Guerchais, K. Kamada, *Polyhedron*, 2018, **140**, 116.

31 A. Scarpaci, C. Monnereau, N. Hergué, E. Blart, S. Legoupy, F. Odobel, A. Gorfo, J. Pérez-Moreno, K. Clays, I. Asselberghs, *Dalton Trans.,* 2009, 4538.

32 A. Colombo, C. Dragonetti, D. Marinotto, S. Righetto, D. Roberto, S. Tavazzi, M. Escadeillas, V. Guerchais, H. Le Bozec, A. Boucekkine, C. Latouche, *Organometallics,* 2013, **32**, 3890.

33 E. Rossi, A. Colombo, C. Dragonetti, S. Righetto, D. Roberto, R. Ugo, A. Valore, J. A. G. Williams, M. G. Lobello, F. De Angelis, S. Fantacci, I. Ledoux-Rak, A. Singh, J. Zyss, *Chem. Eur. J.,* 2013, **19**, 9875.

34 J. Boixel, V. Guerchais, H. Le Bozec, D. Jacquemin, A. Amar, A. Boucekkine, A. Colombo, C. Dragonetti, D. Marinotto, D. Roberto, S. Righetto, R. De Angelis, *J. Am. Chem. Soc.,* 2014, **136**, 5367.

35 J. Boixel, V. Guerchais, H. Le Bozec, A. Chantzis, D. Jacquemin, A. Colombo, C. Dragonetti, D. Marinotto, D. Roberto, *Chem. Commun*., 2015, **51**, 7805.

36 F. Nisic, E. Cariati, A. Colombo, C. Dragonetti, S. Fantacci, E. Garoni, E. Lucenti, S. Righetto, D. Roberto, J.A.G. Williams, *Dalton Trans*., 2017, **46**, 1179.

37 N. Baggi, E. Garoni, A. Colombo, C. Dragonetti, S. Righetto, D. Roberto, J. Boixel, V. Guerchais, S. Fantacci, *Polyhedron*, 2018, **140**, 74.

38 B. F. Levine, C. G. Bethea, *Appl. Phys. Lett.,* 1974, **24**, 445.

39 B. F. Levine, C. G. Bethea, *J. Chem. Phys.,* 1975, **63**, 2666.

40 I. Ledoux, J. Zyss, *Chem. Phys.,* 1982, **73**, 203.

41 A. Valore, M. Balordi, A. Colombo, C. Dragonetti, S. Righetto, D. Roberto, R. Ugo, T. Benincori, G. Rampinini, F. Sannicolò, F. Demartin, *Dalton Trans.,* 2010, **39**, 10314.

42 R. Sharma, N. Patel, R. A. Vishwakarma, P. V. Bharatam and S. B. Bharate, *Chem. Commun.,* 2016, **52**, 1009.

43 M. Vojtičková, J. Dobiaš, G. Hanquet, G. Addová, R. Cetin-Atalay, D. C. Yildirim and A. Boháč, *Eur. J. Med. Chem.,* 2015, **103**, 105.

44 W. Wu, C. Cheng, W. Wu, H. Guo, S. Ji, P. Song, K. Han, J. Zhao, X. Zhang, Y. Wu and G. Du, *Eur. J. Inorg. Chem.*, 2010, **29**, 4683.

45 Q. Zhou, B. Zhang, L. Su, T. Jiang, R. Chen, T. Du, Y. Ye, J. Shen, G. Dai, D. Han and H. Jiang, *Tetrahedron*, 2013, **69**, 10996–11003.

46 D. Marinotto, R. Castagna, S. Righetto, C. Dragonetti, A. Colombo, C. Bertarelli, M. Garbugli, G. Lanzani, *J. Phys. Chem. C* 2011, **115**, 20425.

47 W.N. Herman, L.M. Hayden, *J. Opt. Soc. Am. B,* 1995, **12**, 416.

48 M.J. Frisch, M. J *et al.* Gaussian 16 Revision A.03, 2016, Gaussian Inc. Wallingford CT

49 Y. Zhao, D. G. Truhlar, *Theor. Chem. Acta*, 2008,**120**, 215.

50 D. Jacquemin, E.A. Perpète, I. Ciofini, C. Adamo, R. Valero, Y. Zhao, D.G. Truhlar, *J. Chem. Theory Comput.* 2010, **6**, 2071.

51 J. D. Chai, M. Head-Gordon, *Phys. Chem. Chem. Phys.* 2008, **10**, 6615.

52 J. Tomasi, B. Mennucci, R. Cammi, *Chem. Rev.* 2005, **105**, 2999.

53 A. F. Henwood, A. K. Bansal, D. B. Cordes, A. M. Z. Slawin, I. D. W. Samuel and E. Zysman-Colman, *J. Mater. Chem. C*, 2016, **4**, 3726.

54 S. Ladouceur, D. Fortin and E. Zysman-Colman, *Inorg. Chem.*, 2011, **50**, 11514–11526.

55 R. D. Costa, E. Ortí, D. Tordera, A. Pertegás, H. J. Bolink, S. Graber, C. E. Housecroft, L. Sachno, M. Neuburger and E. C. Constable, *Adv. Energy Mater*., 2011, **1**, 282–290.

56 K. J. Suhr, L. D. Bastatas, Y. Shen, L. A. Mitchell, G. A. Frazier, D. W. Taylor, J. D. Slinker and B. J. Holliday, *Dalton Trans.,* 2016, **45**, 17807.

57 V. Alain, M. Blanchard-Desce, I. Ledoux-Rak, J. Zyss, *Chem. Commun*. 2000, **5**, 353.

58 F. Tessore, E. Cariati, F. Cariati, D. Roberto, R. Ugo, P. Mussini, C. Zuccaccia and A. Macchioni, *ChemPhysChem.,* 2010, **11**, 495.

59 D. R. Kanis, P. G. Lacroix, M. A. Ratner and T. J. Marks, *J. Am. Chem. Soc.,* 1994, **116**, 10089**.**

60 C. Dragonetti, A. Colombo, M. Fontani, D. Marinotto, F. Nisic, S. Righetto, D. Roberto, F. Tintori, S. Fantacci, *Organometallics*, 2016, **35**, 1015.

61 A. Colombo, C. Dragonetti, D. Marinotto, S. Righetto, G. Griffini, S. Turri, H. Akdas-Kilig, J.-L. Fillaut, A. Amar, A. Boucekkine, C. Katan, *Dalton Trans.,* 2016, **45**, 11052.

62 K. Senthilkumar, K. Thirumoorthy, C. Dragonetti, D. Marinotto, S. Righetto, A. Colombo, M. Haukka, N. Palanisami, *Dalton Trans.,* 2016, **45**, 11939.

